

INFLUENCE OF THE BEAM INTENSITY ON THE DESIGN OF THE CERN PS BOOSTER

U. Bigliani, C. Bovet, H.G. Hereward, I. Gumowski, P.L. Morton\*,  
G. Nassibian, K.H. Reich, K. Schindl

S U M M A R Y

The 800 MeV four-ring CERN Proton Synchrotron Booster (PSB) has been designed for accelerating  $10^{13}$  protons per pulse with a high phase space density.

In transverse phase space, this design aim strongly influenced the choice of the nominal beam emittances and of the working point in the  $Q_H - Q_V$  diagram, and led to providing extra aperture, and both normal and skew correction quadrupole as well as sextupole and octupole lenses to deal notably with various linear resonances, with possible throbbing beam instabilities, and with a space-charge induced fourth order coupling resonance.

In longitudinal phase space the high intensity causes in particular a reduction of the effective acceptance area, to be offset by a 20% increase of RF voltage, and calls for more stringent stability tolerances of the RF accelerating system.

The results of the pertinent studies are presented together with some further considerations on the preservation of phase space density.

---

\*) Stanford Linear Accelerator Center.

## 1. Introduction

The design of the four-ring CERN PSB<sup>1,2,3)</sup> has been markedly influenced by the effects of space charge forces and beam-RF cavity interaction at the design intensity of  $10^{13}$  protons per pulse. In contrast, with the machine layout chosen<sup>1)</sup>, no particular problems seem to arise as regards the radiation damage expected<sup>4)</sup>, provided modern technology is used.

## 2. Transverse phase space

In order to increase the 50 MeV Laslett<sup>5)</sup> space charge limit per ring by a factor of 2.5 (i.e. a total increase of 10), and assuming an improvement of the bunching factor by  $\frac{3}{2}$  (Fig. 4), the PSB emittance was chosen as  $E_{\text{PSB}} = \frac{5}{3} E_{\text{CPS}}$ <sup>1)</sup>. (This increases the PSB vertical aperture by 10% compared with the requirement of the Linac emittance alone. Nevertheless an effort is being made to preserve highest phase space density both in the Linac and in the transport channel Linac-PSB<sup>6)</sup>.) The vacuum chamber cross-sections remain comparable because of the PSB betatron wavelength of 35 m as compared to 100 m for the CPS.

At injection the individual particle space charge detuning<sup>5)</sup> amounts to  $\Delta Q_{\text{sc}} = -0.18$  and the coherent space charge detuning to  $\Delta Q_{\text{c}} = -0.12$  for nominal intensity and emittances. If higher intensities or smaller emittances are desired, we must accommodate higher values of  $\Delta Q_{\text{sc}}$  i.e. we must make more room in the working diamond (Fig. 1) by further narrowing the stopband widths. Correction quadrupole lenses are planned<sup>7)</sup> for dealing with the  $2Q_{\text{H,V}} = 9$  resonances simultaneously (necessary in the presence of space charge even if only one resonance is crossed<sup>8)</sup>), and skew quadrupoles for tackling the linear sum and difference resonances<sup>7)</sup>. The space-charge induced difference resonance  $2Q_{\text{H}} - 2Q_{\text{V}} = 0$  will be dealt with by working with a Q-split  $Q_{\text{V}} - Q_{\text{H}} \approx 0.2$ <sup>9)</sup> and using octupoles for compensation of the average space-charge coupling term<sup>7)</sup>. However, the octupole action will also cause some positive amplitude dependent Q-shift.

The cubic and fourth order resonances may be studied, though not cured, by means of the sextupoles and octupoles foreseen<sup>7)</sup>. It is planned to keep the working point away from the crossing points of these resonances marked by full circles on Fig. 1. Our rather low ratio  $\omega_{\text{synchr.}}/\omega_{\beta\text{tron}} < 10^{-3}$  should prevent significant satellite stop bands. In addition some extra working space can be provided through making simultaneously  $dQ_{H,V}/do \approx 0$  by means of the sextupoles, positioned in a straight section with the correct  $\beta_V/\beta_H$  ratio (Fig. 2).

As regards the throbbing beam instabilities, the ion-induced symmetrical (monopole) mode has a growth time of  $\tau = 0.1\text{s}$  for  $10^{-7}$  Torr vacuum pressure<sup>10)</sup>, and damping occurs if the "external" Q spread  $\Delta Q_e > \Delta Q_{sc}/2$ . For  $\omega_{\beta\text{tron}} = \text{const.}$  the dipole mode is stable for  $4 < Q < 4.85$  but Landau damping is probably excluded<sup>11)</sup> because it requires  $\Delta Q_e > \Delta Q_{sc}$ . The quadrupole mode is stable<sup>11)</sup> for  $4 < Q < 4.39$  and  $4.5 < Q < 4.89$ , in any case quadrupole and higher modes are damped for  $\Delta Q_e > \Delta Q_{sc}/4$ . The sextupoles or octupoles already mentioned could possibly be used for providing the required  $\Delta Q_e$ .

The choice of the working point included considering the spread of betatron frequencies due to momentum, amplitude and space charge. Taking into account also the desired Q-split and the stable regions for throbbing modes, we have designed the main quadrupoles for  $Q_H = 4.55$ ,  $Q_V = 4.70$ . Without changing the polarity of the auxiliary power supplies of these quadrupoles one can move the working point inside the small upper right hand rhomb of Fig. 1 at 800 MeV, and five times as far at injection. The upper triangular region seems to be the more favourable one, but the lower (dashed) triangle may also be used; with other polarities of the power supply further regions can be explored. The entire diamond  $4 < Q < 5$  is free of systematic resonances<sup>1)</sup>.

### 3. Longitudinal phase space

#### 3.1 Longitudinal acceptance and trapping in the presence of space charge

In the absence of space charge an RF voltage of 10 kV is required for providing the specified longitudinal acceptance area of  $1.35 \times \text{Linac}$

beam emittance. Using Ref. 12, 13 which give the reduction of acceptance as a function of beam current, we find that for the design intensity the RF voltage must be increased by 20% to offset the reduction of about 10 to 15% both at injection ( $V_{RF} = 12$  kV,  $\phi_s = 4.8^\circ$ ,  $\gamma = 1.05$ ) and transfer ( $V_{RF} = 2.5$  kV,  $\phi_s = 0^\circ$ ,  $\gamma = 1.85$ ).

The process of adiabatic bunching at injection (with a given rising RF voltage) has been followed with a step by step computer calculation taking into account these space charge forces<sup>14)</sup>. The corresponding maximum stable phase plane trajectories for 0,  $2.5 \times 10^{12}$  and  $10^{13}$  protons per ring are shown in Fig. 3 and the change of the PSB and CPS bunching factors with time in Fig. 4.

### 3.2 RF accelerating system

The presence of intense beam loading, by interacting with the cavity tuning, AVC and beam control, adds further feedback paths<sup>15)</sup> to the overall beam control system<sup>16)</sup>. We plan to neutralize the direct influence of the beam phase oscillations on the RF phase (of the same order as via the "normal" path) by an appropriate choice of the phase lock characteristics. Similarly, the AVC will be designed to reduce the (small) term arising from the coupling between phase and voltage amplitude and be made insensitive against the voltage waveform<sup>17)</sup>. Particular attention will be paid to the bunch shape control<sup>18,19)</sup>, to minimize the effect of the oscillation of the beam current fundamental. To obtain deeper insight into the functioning of this multi-loop system, a dynamical mathematical model of sufficient complexity (if the AVC and tuning loops are of order two, the total differential system is of order 19) to retain all essential features of the real system is being developed and studied<sup>20)</sup>.

Depending on the choice of ferrite, a detuning<sup>21)</sup> of the PSB cavities of up to  $60^\circ$  may be required to allow for the reactive component of the beam current, and this will be taken into account in deciding on tuning range, maximum tuning rate and cut-off frequency of the saturation system.

In order to maintain good control of the gap voltage under all conditions of beam loading it was decided to locate a power amplifier of sufficient capacity at the cavity<sup>22)</sup>. Some degree of local feedback may have to be introduced to reduce the amplifier output impedance.

In view of the rather weak longitudinal RF focusing (maximum energy gain/turn 12 keV) it will be necessary to watch very carefully any possible sources of perturbing RF fields. For instance, we study the possibility of reducing the RF voltage induced across the 100 insulating joints in the vacuum pipe of each ring by bridging them with appropriate condensers.

#### 4. Conclusions

The design intensity of the PSB is beyond the threshold where collective phenomena become noticeable. While their consideration influenced substantially (and rendered more difficult and expensive in comparison with a low intensity machine) the design of the PSB, detailed studies so far have not revealed any excessive difficulties.

#### Acknowledgements

This paper benefitted from discussions with W. Hardt, B.W. Montague, W. Schnell and D. Zanaschi. It is a pleasure to thank G. Brianti for his continued interest and support.

#### Distribution

List MPS-SI/1

References

1. C. Bovet and K.H. Reich, A Four-Ring Vertically Stacked 800 MeV Booster Injector for the CERN Proton Synchrotron, MPS/Int. DL/B 67-13 and Proc. 1967 Int. Acc. Conf. Cambridge, 315.
2. K.H. Reich, The CERN Proton Synchrotron Booster, SI/Int. DL/69-1 and Proc. 1969 US Particle Acc. Conf. (Trans. Nucl. Sci., June 1969).
3. G. Brianti et al., Accelerator Data Sheets prepared for this Conference.
4. F. Hoyer, Estimation of Beam Losses and Radiation Dose to Components in the CPS Booster (PSB), SI/Int. DL/69-6.
5. L.J. Laslett, BNL 7534, p. 325 (1963).
6. T.R. Sherwood and C.S. Taylor, private communication.
7. C. Bovet and K.H. Reich, Correcting magnets for the PSB: their choice, location and performance specifications, SI/Int. DL/69-3.
8. D. Möhl and L. Thorndahl, Crossing of Half Integer Stop-Bands, an Experimental Study Performed on the CPS, ISR-300/LI/GS/69-20.
9. B.W. Montague, Fourth-Order Coupling Resonance Excited by Space-Charge Forces in a Synchrotron, CERN 68-38.
10. H.G. Hereward, P.L. Morton and K.H. Schindl, The Effect of Ions on the Symmetrical Throbbing Beam Mode, MPS-SI/Int. DL/68-4 and Proc. 1969 US Particle Acc. Conf.
11. P.L. Morton, An Investigation of Space Charge Effects for the Booster Injector to the CPS, SI/Int. DL/68-3.
12. C. Bovet et al., A Selection of Formulae and Data Useful for the Design of A.G. Synchrotrons, MPS-SI/Int. DL/68-3, Fig. III.3.2.2.
13. C.E. Nielsen and A.M. Sessler, Longitudinal Space Charge Effects in Particle Accelerators, RSI 30, 80 (1959) (as corrected in Ref. 11).
14. U. Bigliani, Système HF du Booster, capture dans l'espace de phase longitudinal, SI/Int. EL/68-2.
15. G. Rees, Calculated Beam-Loading Effects in the NAL Main Ring RF system, Proc. 1969 US Particle Acc. Conf. (Trans. Nucl. Science, June 1969).
16. U. Bigliani, Progress Report on PSB Beam Control, SI/Int. EL/69-1.
17. H.H. Umstätter, Elimination of a Beam Loading Effect at Transition and during Debunching on the AVC of the PS Cavities, MPS/Int. SR/69-8.

18. H.G. Hereward, Second-Order Effects in Beam-Control Systems of Particle Accelerators, Proc. 1961 Int. Acc. Conf. New-York, 236.
19. E.C. Raka, Damping Bunch Shape Oscillations in the Brookhaven AGS, Proc. 1969 US Particle Acc. Conf.
20. I. Gumowski, CERN Internal Report to be issued.
21. G. Nassibian, Cavity Loading by Fundamental Component of Beam Current, SI/Note EL/69-5.
22. G. Nassibian, K.H. Reich and D. Zanaschi, Emplacement de l'étage de puissance de l'amplificateur HF du système d'accélération du PSB, SI/Note EL/69-2.
23. K. Johnsen, High Trapping Efficiency in Synchrotrons with Phase Lock, Proc. 1961 Int. Acc. Conf. New-York, 194.

List of Figures

- Fig. 1  $Q_H, Q_V$  diagram of PSB with two (triangular) working regions. Dashed rhombs show the tuning range at 800 MeV, full circles indicate the crossing of the cubic and fourth order resonance lines.
- Fig. 2 PSB lattice with extreme values of beta functions in the tuning range  $4.1 < Q_{H,V} < 4.9$ , and their ratio.  
B = bending magnet,  
F,D = main quadrupoles,  
M = correction multipoles.
- Fig. 3 Deformation of the PSB bucket due to space charge 600  $\mu$ s after injection.
- Fig. 4 Change of present CPS and future PSB bunching factors during longitudinal capture at 50 MeV.





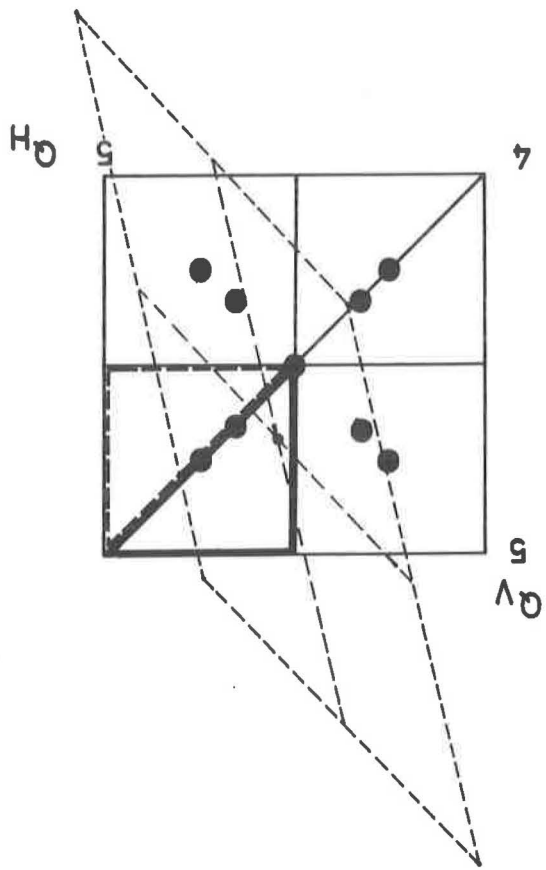


FIG. 1.

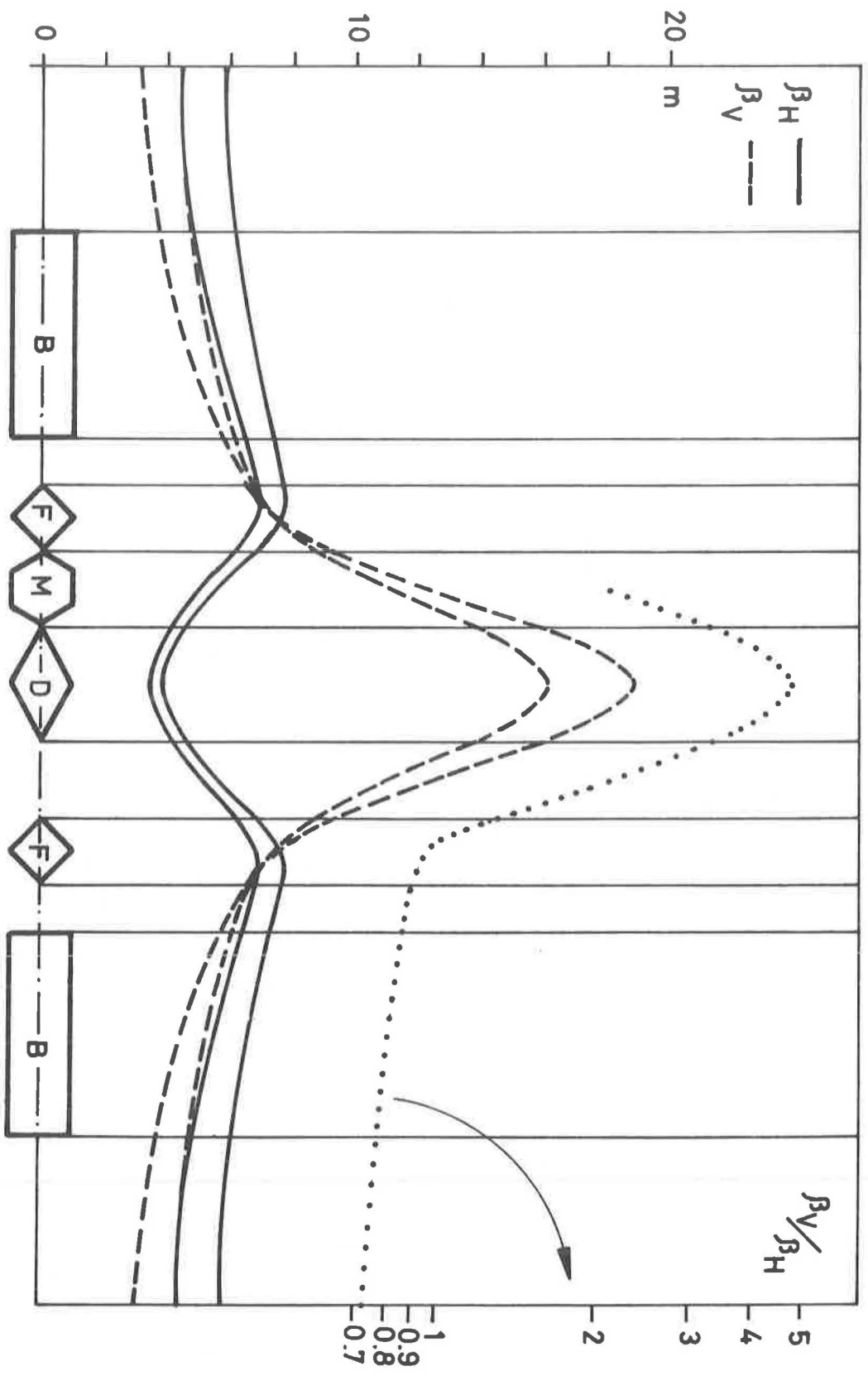


FIG. 2 -

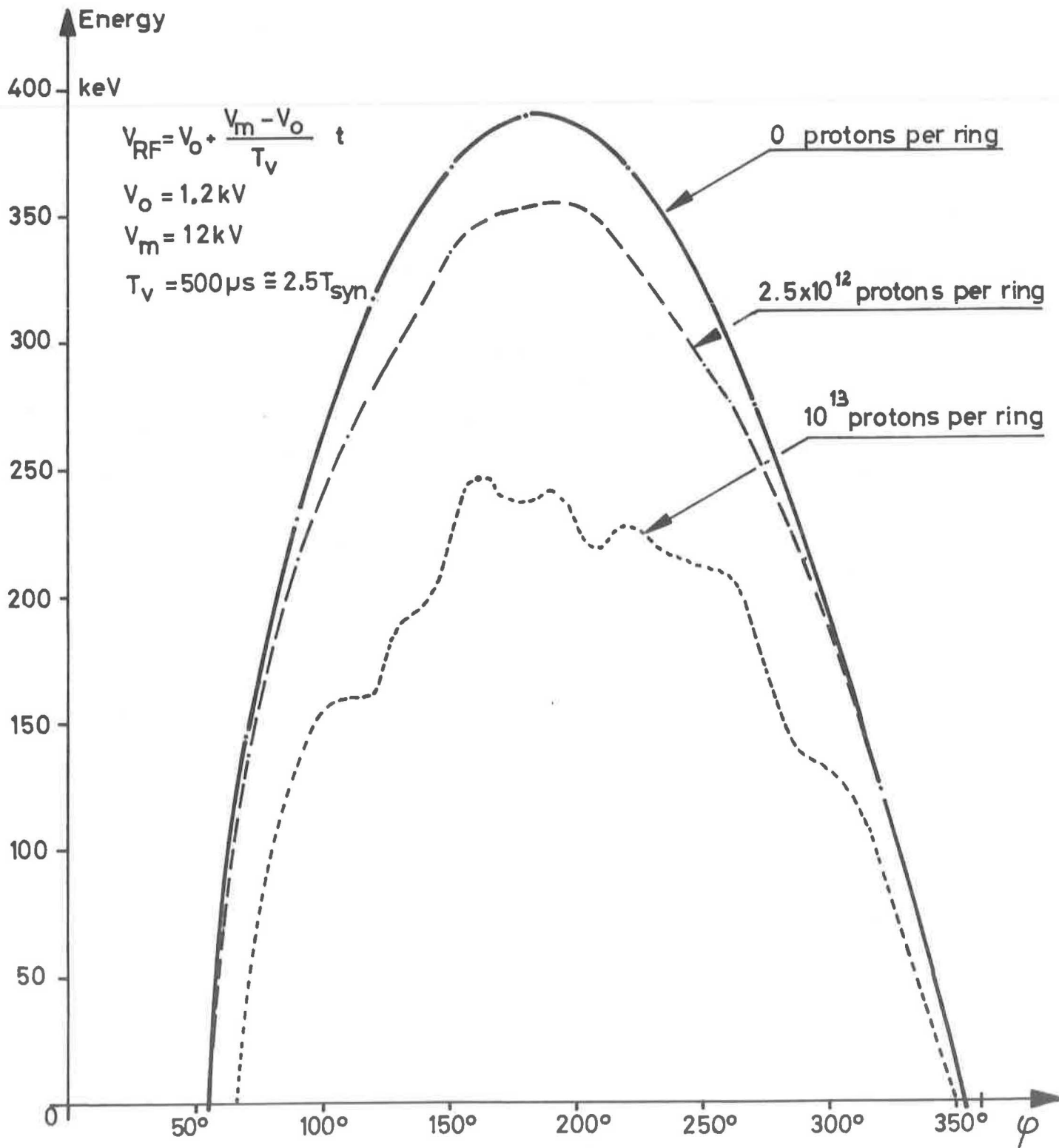
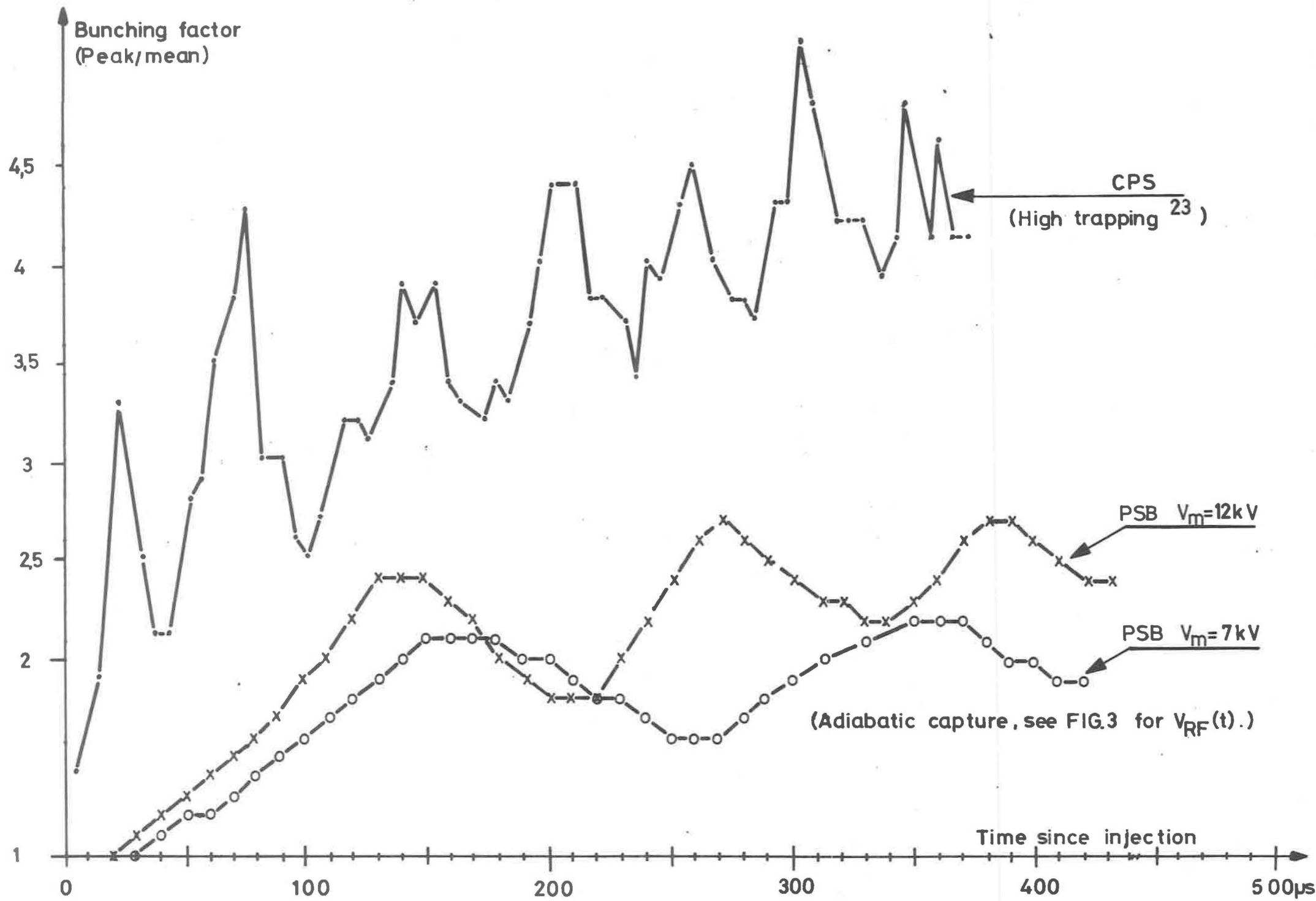


FIG. 3\_



**FIG. 4-**